INTERNATIONAL JOURNAL FOR NUMERICAL AND ANALYTICAL METHODS IN GEOMECHANICS
Int. J. Numer. Anal. Meth. Geomech. (in press)
Published online in Wiley InterScience (www.interscience.wiley.com). DOI: 10.1002/nag.636

Settlements and stresses of multi-layered grounds and improved grounds by equivalent elastic method

Hiroyoshi Hirai*, †

Applied Geotechnical Institute, Inc., Oizumi, Hokuto, Yamanashi 409-1502, Japan

SUMMARY

The investigation of equivalent elastic method is made to predict settlements and stresses of multi-layered grounds and improved grounds. Analytical models to represent the heterogeneous elastic properties of layers in vertical and horizontal directions for multi-layered grounds and improved grounds are proposed in taking into account the equivalent elastic modulus and the equivalent thickness. By introducing the equivalent thickness derived from Terzaghi's formula of the vertical stress, the equivalent elastic method of using the equivalent elastic modulus and the equivalent thickness is applied to the formulations concerning immediate settlements and vertical stresses in multi-layered grounds and improved grounds. Comparison is performed between rigorous solutions and simulations for immediate settlements and vertical stresses in multi-layered grounds and improved grounds. It is found that the proposed method is able to describe properly the characteristics of distributions for settlements and vertical stresses in multi-layered grounds and improved grounds. Copyright © 2007 John Wiley & Sons, Ltd.

Received 15 September 2006; Revised 11 February 2007; Accepted 3 May 2007

KEY WORDS: immediate settlement; vertical stress; equivalent elastic method; multi-layered grounds; improved grounds

INTRODUCTION

Concerning design methods for foundations of structures, a great attention has been focused not only on the bearing capacity but also on settlements and stresses below the foundation under various loading conditions recently. Conventional methods based on the allowable stress design and the limit state design have been often utilized in designs of building's foundations. It has been required that deformations and stresses developed in a structure due to service loads have to be predicted more accurately in design methods. Numerical analyses such as the finite element

*Correspondence to: Hiroyoshi Hirai, Applied Geotechnical Institute, Inc., Oizumi, Hokuto, Yamanashi 409-1502, Japan.
†E-mail: ojiken@eps4.comlink.ne.jp

method (FEM) and the boundary element method (BEM) have provided accurately settlements and stresses beneath foundations for multi-layered soil systems or multi-layered soil systems with soil improvement if the formulation employed establishes efficiently constitutive models into which detailed stress–strain relationships can be incorporated. For application to numerical analyses of FEM and BEM, Hirai [1–3], Kamei and Hirai [4], Hirai and Kamei [5], Hirai *et al*. [6] proposed constitutive models of sandy soils, cohesive soils and improved soils to describe the characteristics of elastic–plastic behaviours in general stresses. For practical designs of building's foundations, however, conventional methods [7, 8] which adopt closed-form linear elastic solutions have not yet been superseded by FEM and BEM due to availability and simplicity of conventional methods. Because of this reason, special efforts are made to derive the formulation of immediate settlements and vertical stresses which possess closed-form linear elastic solutions for both multi-layered soil systems and multi-layered soil systems with soil improvement. In addition, the consolidation settlements classified as elastic–plastic deformation are calculated by use of vertical stresses aforementioned.

Regarding settlements and stresses of multi-layered soil systems, Burmister [9–13] and Fox [14] provided rigorous solutions for two-layered elastic systems and Burmister [9–13], Schiffman [15], Kirk [16] and Jones [17] revealed exact solutions for three-layered elastic systems. For the immediate settlement classified as elastic deformation in soil–rock system, Ueshita and Meyerhof [18] exhibited the rigorous solutions which were employed to verify the availability of approximate solutions calculated by Steinbrenner's [19, 20] method. Furthermore, as for the immediate settlement of multi-layered soil systems, Ueshita and Meyerhof [21, 22] presented the rigorous solutions with which the approximate solutions given by Odemark's [23] method was compared. Palmer and Barber [24] proposed the approximate solution for two-layered elastic systems by the use of the equivalent thickness. Using computational results provided by Burmister [9–13], Nascimento *et al*. [25] propounded an approximate analytical method for pavements of multi-layered systems. In Palmer *et al*.'s method and Odemark's method, it is assumed that once multi-layered elastic systems with n-layers have been transformed into an equivalent single elastic layer, the calculation is only valid within the lowest layer n which is an isotropic and homogeneous material. Ullidtz [26] and Freeman and Harr [27] presented that Odemark's method is able to approximate the multilayer theory of elasticity only for the case where elastic moduli of layers decrease with depth.

Using a simple extrapolation of Steinbrenner's approximation that the compression of a finite layer of depth z metres on a rigid base is the same as the compression within the top z metres of an infinitely deep deposit, Simons and Menzies [28] proposed an approximate method which accommodates a variation of the elastic modulus with depth by replacing each real layer in multi-layered soil systems with one hypothetical layer on a rigid base. Simons *et al*.'s method was utilized in the case where elastic moduli within these layers increase with depth and it was adopted in Recommendations for Design of Building Foundations [7, 8] published by the Architectural Institute of Japan. By weighting the elastic parameters of each layer in a multi-layered system, Fraser and Wardle [29] provided an equivalent elastic modulus which is same as the elastic modulus derived from the extrapolation of Steinbrenner's approximation. Poulos and Davis [30] indicated that the use of extrapolation of Steinbrenner's approximation for a multi-layered system leads to an overestimate of settlement caused by the underlying layers if the modulus of the layers decreases with depth. It was shown by Hirai and Kamei [31, 32] that the settlement obtained by the extrapolation of Steinbrenner's approximation is not applicable to the case where elastic moduli within multi-layered soil systems decrease with depth. Himeno [33] and

DOI: 10.1002/nag

Matsui [34] presented computational programs which analyse settlements, stresses and strains generally in multi-layered elastic systems. The computational programs by Himeno and Matsui, however, are employed only for circular loads but not for rectangular loads on the surface in multi-layered soil systems.

In the following presentation, the investigation is made to propose the equivalent elastic method which consists of equivalent elastic modulus and equivalent thickness [31, 32] for multi-layered soil systems with soil improvement. First, both improved soil columns and internal soil layers surrounded with improved soil columns are transformed into a composite soil system with the equivalent elastic modulus. Second, the composite soil system and external soil layers are transformed into equivalent multi-layered soil systems. The analytical method which includes the equivalent elastic modulus and the equivalent thickness is exhibited by developing the approximate solutions given by Palmer and Braber [24], Odemark [23] and Terzaghi [35].

The investigation is performed for the influence of loaded area, both area and depth of soil improvements, and the difference of elastic moduli between *in situ* soils and improved soils upon settlements and stresses of improved soil systems. In comparison with rigorous solutions, finite element analysis and multi-layer elastic analysis, the applicability of the proposed method is demonstrated.

In the computation for consolidation settlements of cohesive soils, Hirai and Kamei [36, 37] proposed analytical methods to estimate the consolidated state and the consolidation yield stress. It is very important that distributions of vertical stress in soil systems have to be determined precisely in the calculation of consolidation settlements. In the following presentation, two analytical methods of vertical stresses in multi-layered soil systems are utilized; i.e. the direct method to use the equivalent thickness directly and the indirect method of adopting distribution widths of vertical stresses expressed with equivalent thickness.

EQUIVALENT THICKNESS AND EQUIVALENT ELASTIC MODULUS OF MULTI-LAYERED SOIL SYSTEMS

In the case of three-dimensional elastic problems to satisfy boundary conditions with complicated shapes in an infinite solid, Hirai and Satake [38, 39] proposed the analytical method of utilizing transformations between functions in cylindrical coordinates and those in spherical ones. For three-dimensional elastic problems encountered in multi-layered soil systems, it becomes more difficult to satisfy accurately the boundary conditions between each layer in proportion to increase in soil layers because of the complication of integrations [21, 22, 34] included in three-dimensional elastic analyses. Furthermore, the three-dimensional elastic analyses for rectangular foundations have a tendency to become more complicated than circular foundations. In order to predict settlements and stresses under vertical loadings on multi-layered soil systems, Hirai and Kamei [31, 32] proposed approximate analytical procedures to develop the methods given by Palmer and Barber [24] and Odemark [23].

Figure 1 exhibits multi-layered soil systems composed of n-layers subjected to vertical loads q. As shown in Figure 1, the present procedure uses the elastic moduli, i.e. Young's modulus E_m and Poisson's ratio ν_m and thickness H_m for mth layer in n-layers of multi-layered soil systems, and B and D_f are dimension and depth of a foundation, respectively. According to Palmer and Barber's method [24] for two layers and Odemark's [23] method for multi-layers, the equivalent

DOI: 10.1002/nag

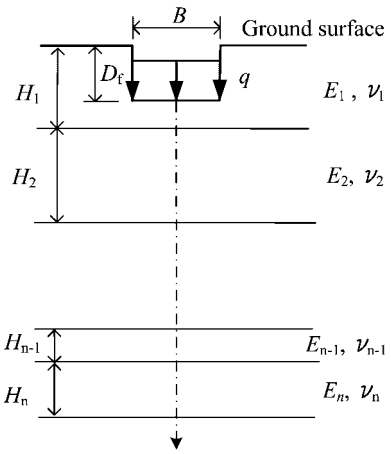

Figure 1. Multi-layered soil systems.

thickness H_{me} was given by the following expression: for the case where $E_m \geqslant E_n$

$$H_{1e} - D_f = \left\{ \frac{E_1(1-\nu_n^2)}{E_n(1-\nu_1^2)} \right\}^{1/3} (H_1 - D_f)$$
$$H_{me} = \left\{ \frac{E_m(1-\nu_n^2)}{E_n(1-\nu_m^2)} \right\}^{1/3} H_m \quad (m = 2 \sim n) \tag{1}$$

As for the case where $E_m \leqslant E_n$, considering that Terzaghi's [35] approximate formula of the vertical stress is available for a layer on a rigid base, i.e. $E_2 = \infty$ in two layers, it is assumed that the equivalent thickness H_{me} for multi-layers may be represented by an interpolation function as follows:

$$H_{1e} - D_f = \left[0.75 + 0.25 \left\{ \frac{E_1(1-\nu_n^2)}{E_n(1-\nu_1^2)} \right\}^{1/3} \right] (H_1 - D_f)$$
$$H_{me} = \left[0.75 + 0.25 \left\{ \frac{E_m(1-\nu_n^2)}{E_n(1-\nu_m^2)} \right\}^{1/3} \right] H_m \quad (m = 2 \sim n) \tag{2}$$

Figure 2 shows an equivalent single soil layer with the equivalent thickness expressed by Equations (1) and/or (2) for multi-layered soil systems exhibited in Figure 1. In Figure 2, it is assumed that the vertical stress is distributed with the gradient of $\tan\alpha$ [40] in the case of an isotropic and homogeneous elastic system. The present procedure takes $\tan\alpha = \frac{1}{2}$ [41] for convenience. Therefore, the transverse dimension B_{je} and the longitudinal dimension L_{je} of vertical stress

DOI: 10.1002/nag

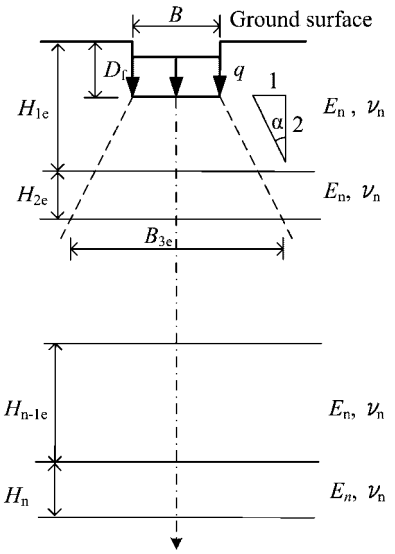

Figure 2. Equivalent single soil layer with equivalent thickness for Figure 1.

distributed on the upper boundary of jth layer were given by the following form [32]:

$$\begin{aligned} B_{1e} &= B, \quad B_{je} = B - D_f + \sum_{k=1}^{j-1} H_{ke} \ \ (j \neq 1) \\ L_{1e} &= L, \quad L_{je} = L - D_f + \sum_{k=1}^{j-1} H_{ke} \ \ (j \neq 1) \end{aligned} \tag{3}$$

where B and L are the transverse dimension and the longitudinal dimension of a rectangular foundation, respectively, on the assumption that $B \leqslant L$, and B_{je} and L_{je} are referred to as distribution widths of vertical stress of jth layer.

The n-layered soil systems shown in Figure 3 was transformed into equivalent two-layered soil systems illustrated in Figure 4. The equivalent elastic modulus E_H [31, 32] for $n-1$ layers in Figure 4 was represented by

$$E_H = \left[\left\{ E_1 \frac{(1-\nu_n^2)}{(1-\nu_1^2)} \right\}^{1/3} \frac{H_1 - D_f}{H - D_f} + \sum_{j=2}^{n-1} \left\{ E_j \frac{(1-\nu_n^2)}{(1-\nu_j^2)} \right\}^{1/3} \frac{H_j}{H - D_f} \right]^3 \tag{4}$$

Furthermore, two-layered soil systems in Figure 4 was transformed into an equivalent single soil layer shown in Figure 5 by the use of the equivalent thickness as follows: for the case where $E_H \geqslant E_n$ [31, 32]

$$H_e - D_f = \left(\frac{E_H}{E_n} \right)^{1/3} (H - D_f) \tag{5}$$

DOI: 10.1002/nag

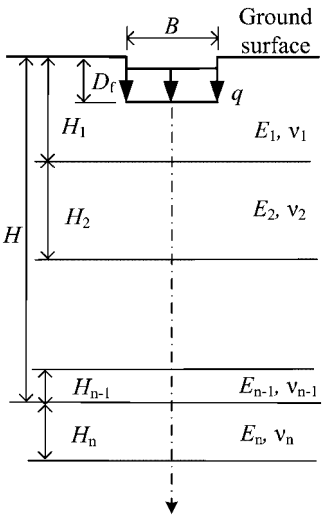

Figure 3. Multi-layered soil systems.

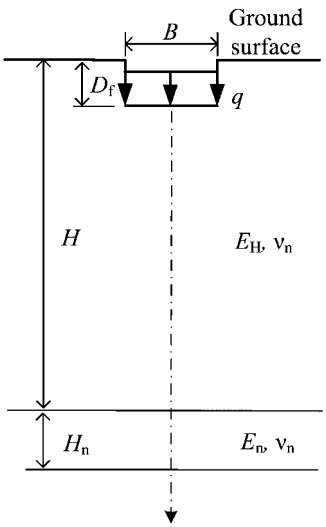

Figure 4. Equivalent two-layered soil systems for Figure 3.

and for the case where $E_H \leqslant E_n$

$$H_e - D_f = \left[0.75 + 0.25\left(\frac{E_H}{E_n}\right)^{1/3}\right](H - D_f) \tag{6}$$

DOI: 10.1002/nag

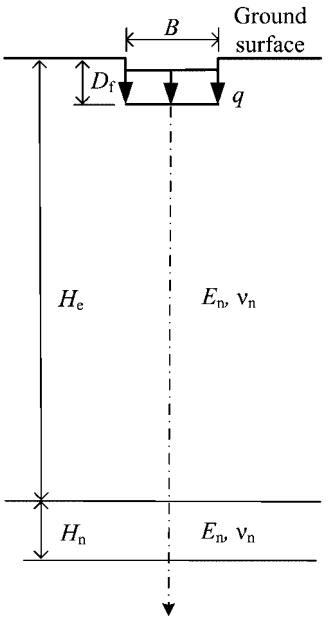

Figure 5. Equivalent single soil layer for Figure 4.

EQUIVALENT THICKNESS AND EQUIVALENT ELASTIC MODULUS OF IMPROVED SOIL SYSTEMS

Figure 6 shows schematically multi-layered soil systems subjected to vertical loads q at depth D_f. Figure 7 illustrates equivalent multi-layered soil systems with equivalent elastic modulus $E_T^{(k-1)}$ for Figure 6. Concerning $k-1$ layers within multi-layered soil systems shown in Figure 6, the equivalent elastic modulus $E_T^{(k-1)}$ illustrated in Figure 7 can be expressed by Equation (4) where n is replaced with k. Figure 8 exhibits improved soil systems which are composed of improved soil columns and multi-layered soil systems in the case where soil improvements are achieved for multi-layered soil systems shown in Figure 6. Both improved soil columns and internal soil layers surrounded with improved soil columns in Figure 8 are transformed into a composite soil system with equivalent elastic moduli E_{eq} and υ_{eq} in Figure 9. Figure 9 shows equivalent improved soil systems which consist of the composite soil system and external multi-layered soil systems for Figure 8.

Using the elastic modulus E_p and Poisson's ratio υ_p of improved soil columns, the equivalent elastic modulus E_{eq} and the equivalent Poisson's ratio υ_{eq} for the composite soil system exhibited in Figure 9 were derived as follows [42]:

$$\begin{aligned} E_{eq} &= E_T^{(k-1)} + (E_p - E_T^{(k-1)}) \sum A_p / A_b \\ \nu_{eq} &= \nu_n + (\nu_p - \nu_n) \sum A_p / A_b \end{aligned} \tag{7}$$

DOI: 10.1002/nag

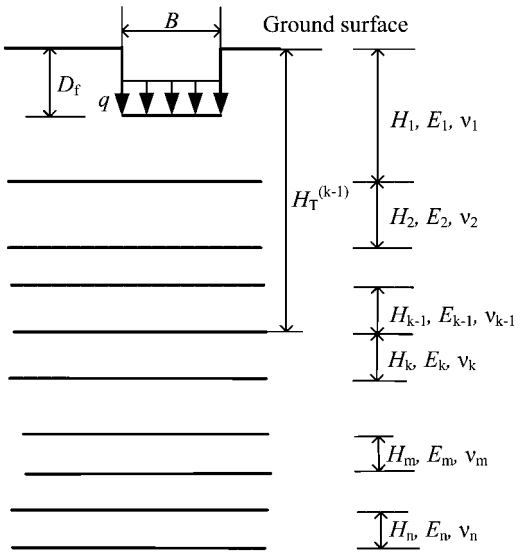

Figure 6. Multi-layered soil systems.

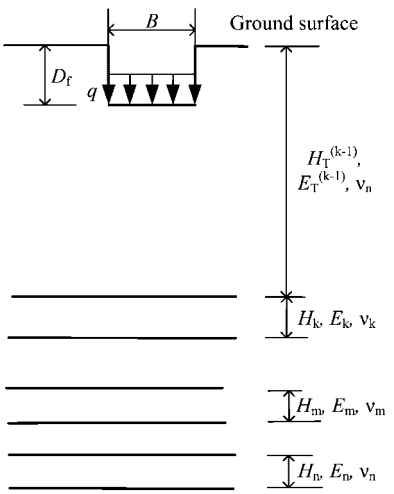

Figure 7. Equivalent multi-layered soil systems with equivalent elastic modulus for Figure 6.

where $\sum A_p$ is the sum of the area of base of improved soil columns, $A_b = B_b L_b$ is the area of base of the composite soil system, and B_b and L_b are the transverse dimension and the longitudinal one of the base of the composite soil system, respectively. The elastic–plastic behaviour of improved sandy soils was investigated by Hirai *et al.* [6] and the method to determine elastic moduli of improved sandy soils was proposed.

DOI: 10.1002/nag

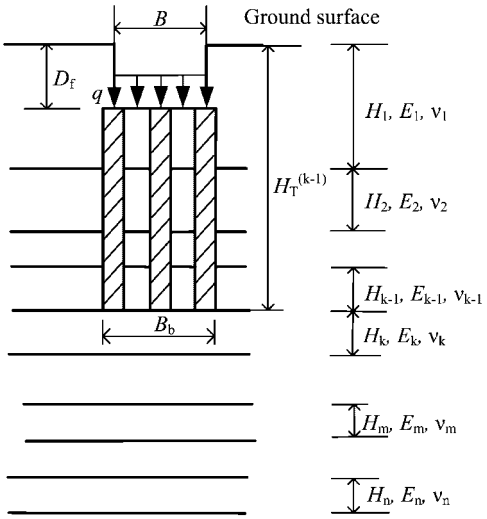

Figure 8. Improved soil systems composed of improved soil columns and multi-layered soil systems for Figure 6.

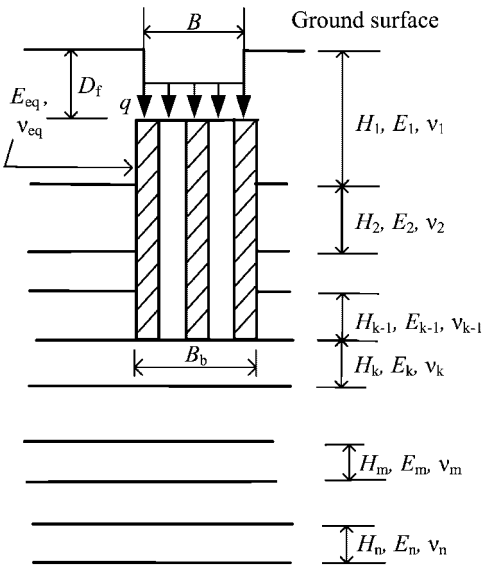

Figure 9. Equivalent improved soil systems composed of a composite soil system and multi-layered soil systems for Figure 8.

Let us consider the case where $k-1$ layers of the upper part of multi-layered soil systems shown in Figure 6 are replaced with the equivalent moduli E_{eq} and υ_{eq}. Figure 10 illustrates that replaced soil systems are composed of both the upper part of $k-1$ layers replaced with the equivalent

DOI: 10.1002/nag

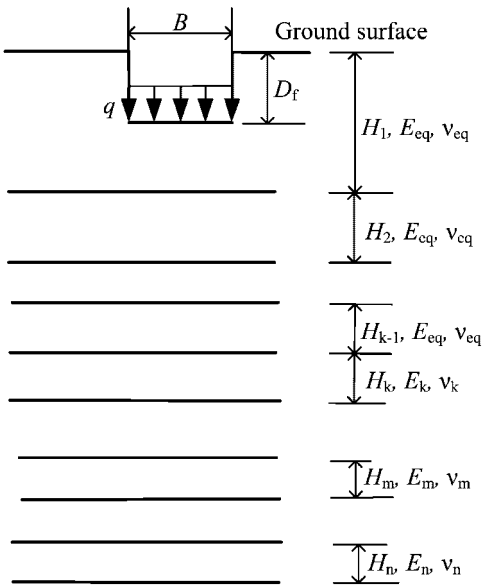

Figure 10. Replaced soil systems composed of both $k-1$ layers replaced with equivalent elastic moduli and $n-k+1$ layers of native soils for Figure 6.

moduli E_{eq} and υ_{eq} and the lower part of $n-k+1$ layers of multi-layered soil systems. Figure 11 exhibits an equivalent single soil layer with equivalent thickness for Figure 10. It is assumed in Figure 11 that the vertical stress is distributed with the gradient of $\tan\alpha = \frac{1}{2}$ in an isotropic and homogeneous elastic system. Therefore, the transverse dimension B_{ke} and the longitudinal one L_{ke} of distribution widths of vertical stress on the upper boundary of kth layer are given by the following form:

$$\begin{aligned} B_{ke} &= B - D_f + \sum_{m=1}^{k-1} H_{me} \\ L_{ke} &= L - D_f + \sum_{m=1}^{k-1} H_{me} \end{aligned} \tag{8}$$

where the equivalent thickness of equivalent single soil layer shown in Figure 11 is expressed by the following equations:
for the case where $E_{eq} \geqslant E_n$ [43, 44]

$$\begin{aligned} H_{1e} - D_f &= \left\{ \frac{E_{eq}(1-\nu_n^2)}{E_n(1-\nu_{eq}^2)} \right\}^{1/3} (H_1 - D_f) \\ H_{me} &= \left\{ \frac{E_{eq}(1-\nu_n^2)}{E_n(1-\nu_{eq}^2)} \right\}^{1/3} H_m \quad (m = 2 \sim k-1) \end{aligned} \tag{9}$$

DOI: 10.1002/nag

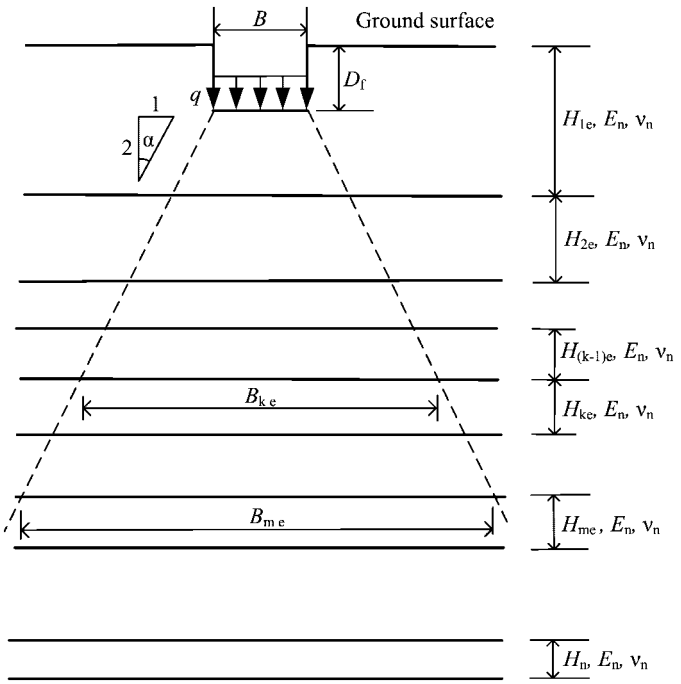

Figure 11. Equivalent single soil layer with equivalent thickness for Figure 10.

for the case where $E_{eq} \leqslant E_n$

$$H_{1e} - D_f = \left[0.75 + 0.25\left\{\frac{E_{eq}(1-\nu_n^2)}{E_n(1-\nu_1^2)}\right\}^{1/3}\right](H_1 - D_f)$$
$$H_{me} = \left[0.75 + 0.25\left\{\frac{E_{eq}(1-\nu_n^2)}{E_n(1-\nu_m^2)}\right\}^{1/3}\right]H_m \quad (m = 2 \sim k-1) \tag{10}$$

for the case where $E_m \geqslant E_n$ [43, 44]

$$H_{me} = \left\{\frac{E_m(1-\nu_n^2)}{E_n(1-\nu_m^2)}\right\}^{1/3} H_m \quad (m = k \sim n) \tag{11}$$

and for the case where $E_m \leqslant E_n$

$$H_{me} = \left[0.75 + 0.25\left\{\frac{E_m(1-\nu_n^2)}{E_n(1-\nu_m^2)}\right\}^{1/3}\right]H_m \quad (m = k \sim n) \tag{12}$$

Figure 12 exhibits distribution widths of vertical stress on each layer shown in Figure 10, in which distribution widths of vertical stress are the same as those shown in Figure 11.

DOI: 10.1002/nag

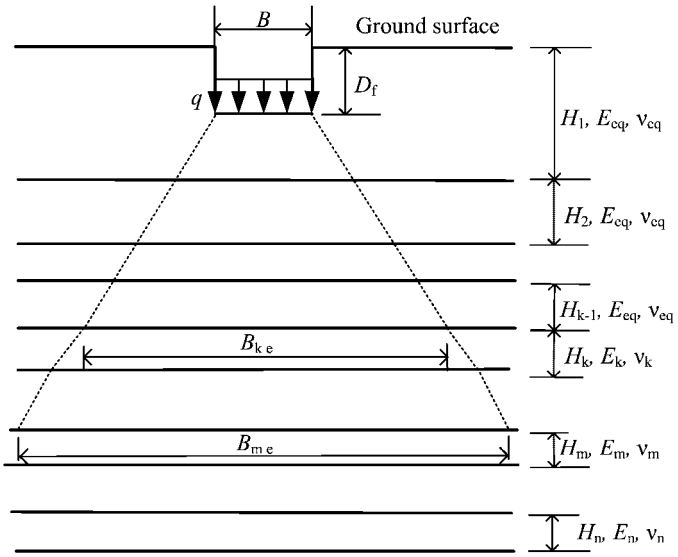

Figure 12. Distribution widths of vertical stress for Figure 10.

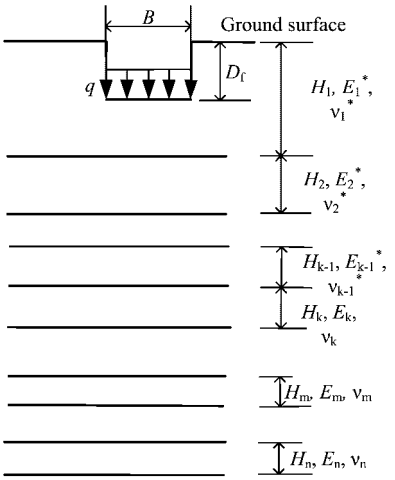

Figure 13. Equivalent multi-layered soil systems with equivalent elastic moduli for Figure 9.

Figure 13 illustrates equivalent multi-layered soil systems with equivalent elastic moduli for improved soil systems shown in Figure 9. Using the equivalent elastic modulus E_{eq} and the equivalent Poisson's ratio υ_{eq} for the composite soil system and the elastic modulus E_m and Poisson's ratio υ_m of multi-layered soil systems exhibited in Figure 9, the equivalent elastic

DOI: 10.1002/nag

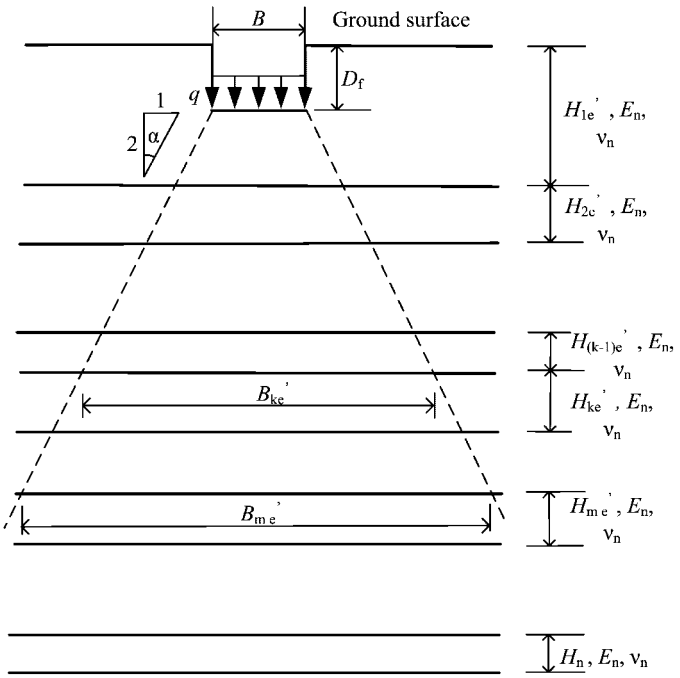

Figure 14. Equivalent single soil layer with equivalent thickness for Figure 13.

moduli in Figure 13 are proposed by making reference to the derivation of Equation (7) as follows:

$$\begin{aligned} E_m^* &= E_m + (E_{\text{eq}} - E_m) B_{\text{b}} L_{\text{b}} / (B_{ke} L_{ke}) \\ v_m^* &= v_m + (v_{\text{eq}} - v_m) B_{\text{b}} L_{\text{b}} / (B_{ke} L_{ke}) \quad (m = 1 \sim k-1) \end{aligned} \tag{13}$$

where if $B_{\text{b}} L_{\text{b}} / (B_{ke} L_{ke}) > 1$, it follows that $B_{\text{b}} L_{\text{b}} / (B_{ke} L_{ke}) = 1$.

Therefore, improved soil systems which are composed of improved soil columns and multi-layered soil systems exhibited in Figure 8 are transformed finally into equivalent multi-layered soil systems with equivalent elastic moduli as shown in Figure 13. Here, since improved soil systems are reduced to the equivalent multi-layered soil systems, the preceding analytical procedures for multi-layered soil systems shown in Figures 1 and 3 are applicable to multi-layered soil systems with transformed elastic moduli indicated in Figure 13.

Figure 14 exhibits the equivalent single soil layer with equivalent thickness for Figure 13. Since it is assumed in Figure 14 that the vertical stress is distributed with the gradient of $\tan\alpha = \frac{1}{2}$ in an isotropic and homogeneous elastic system, the transverse dimension B'_{je} and the longitudinal one L'_{je} of distribution widths of vertical stress on the upper boundary of jth layer are given by the following form:

$$\begin{aligned} B'_{1e} &= B, \quad B'_{je} = B - D_{\text{f}} + \sum_{m=1}^{j-1} H'_{me} \quad (j \neq 1) \\ L'_{1e} &= L, \quad L'_{je} = L - D_{\text{f}} + \sum_{m=1}^{j-1} H'_{me} \quad (j \neq 1) \end{aligned} \tag{14}$$

DOI: 10.1002/nag

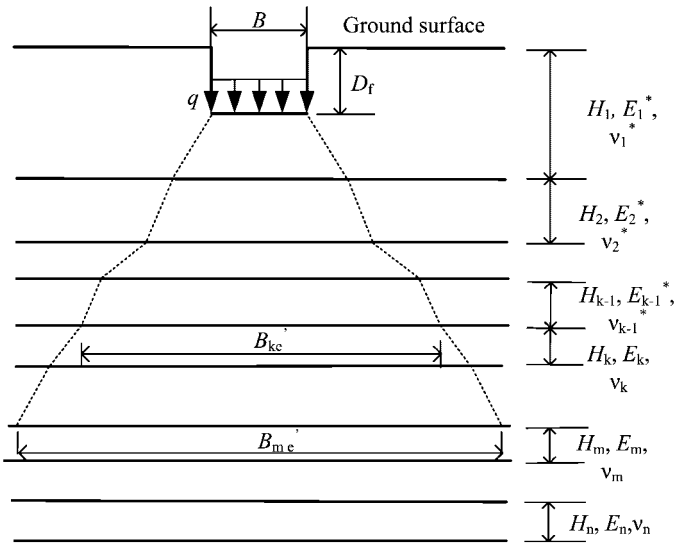

Figure 15. Distribution widths of vertical stress for Figure 13.

where the equivalent thickness of the equivalent single soil layer shown in Figure 14 is expressed by the following equations:

for the case where $E_m^* \geqslant E_n$ [43, 44]

$$H'_{1e} - D_f = \left\{ \frac{E_1^*(1-\nu_n^2)}{E_n(1-\nu_1^{*2})} \right\}^{1/3} (H_1 - D_f)$$
$$H'_{me} = \left\{ \frac{E_m^*(1-\nu_n^2)}{E_n(1-\nu_m^{*2})} \right\}^{1/3} H_m \quad (m = 2 \sim k-1) \tag{15}$$

for the case where $E_m^* \leqslant E_n$

$$H'_{1e} - D_f = \left[0.75 + 0.25 \left\{ \frac{E_1^*(1-\nu_n^2)}{E_n(1-\nu_1^{*2})} \right\}^{1/3} \right] (H_1 - D_f)$$
$$H'_{me} = \left[0.75 + 0.25 \left\{ \frac{E_m^*(1-\nu_n^2)}{E_n(1-\nu_m^{*2})} \right\}^{1/3} \right] H_m \quad (m = 2 \sim k-1) \tag{16}$$

for the case where $E_m \geqslant E_n$ [43, 44]

$$H'_{me} = \left\{ \frac{E_m(1-\nu_n^2)}{E_n(1-\nu_m^2)} \right\}^{1/3} H_m \quad (m = k \sim n) \tag{17}$$

DOI: 10.1002/nag

and for the case where $E_m \leqslant E_n$

$$H'_{me} = \left[0.75 + 0.25 \left\{ \frac{E_m(1-\nu_n^2)}{E_n(1-\nu_m^2)} \right\}^{1/3} \right] H_m \quad (m = k \sim n) \tag{18}$$

Figure 15 exhibits distribution widths of vertical stress on each layer shown in Figure 13, in which distribution widths of vertical stress are the same as those shown in Figure 14.

IMMEDIATE SETTLEMENTS

For the semi-infinite soil medium of the elastic modulus E_n and Poisson's ratio ν_n subjected to uniform loads q on a rectangular foundation with the transverse dimension B and the longitudinal one L, the immediate settlement at the depth z below the centre of foundation is expressed as follows [19, 20]:

$$w(z) = \frac{2Bq(1-\nu_n^2)}{\pi E_n} \left[\log_e \left(\frac{\sqrt{1+m^2+n^2}+m}{\sqrt{1+n^2}} \right) + m \log_e \left(\frac{\sqrt{1+m^2+n^2}+1}{\sqrt{m^2+n^2}} \right) \right.$$
$$\left. - \frac{1-2\nu_n}{2(1-\nu_n)} n \tan^{-1} \left(\frac{m}{n\sqrt{1+m^2+n^2}} \right) \right] = \frac{K(z,\nu_n)}{E_n} Bq \tag{19}$$

where $m = L/B$, $n = 2z/B$ and $K(z, \nu_n)$ is represented as follows:

$$K(z,\nu_n) = \frac{2(1-\nu_n^2)}{\pi} \left[\log_e \left(\frac{\sqrt{1+m^2+n^2}+m}{\sqrt{1+n^2}} \right) + m \log_e \left(\frac{\sqrt{1+m^2+n^2}+1}{\sqrt{m^2+n^2}} \right) \right.$$
$$\left. - \frac{1-2\nu_n}{2(1-\nu_n)} n \tan^{-1} \left(\frac{m}{n\sqrt{1+m^2+n^2}} \right) \right] \tag{20}$$

As for the semi-infinite soil medium of the elastic modulus E_n and Poisson's ratio ν_n subjected to uniform loads q on a circular foundation with radius a, the immediate settlement at the depth z below the centre of foundation is written as follows [45–47]:

$$w(z) = \frac{2aq(1-\nu_n^2)}{E_n} \left(\sqrt{1+\frac{z^2}{a^2}} - \frac{z}{a} \right) \left\{ 1 + \frac{z/a}{2(1-\nu_n)\sqrt{1+\dfrac{z^2}{a^2}}} \right\} = \frac{K(z,\nu_n)}{E_n} Bq \tag{21}$$

where $B = 2a$ and

$$K(z,\nu_n) = (1-\nu_n^2) \left(\sqrt{1+\frac{z^2}{a^2}} - \frac{z}{a} \right) \left\{ 1 + \frac{z/a}{2(1-\nu_n)\sqrt{1+\dfrac{z^2}{a^2}}} \right\} \tag{22}$$

DOI: 10.1002/nag

For the immediate settlement in the centre of a foundation for multi-layered soil systems shown in Figure 1, a modified form of Palmer and Barber's method, which is called the modified Palmer and Barber's method, is proposed in the following form [31, 32]:

$$S_i = \left\{ \frac{I(H_{1e} - D_f, \nu_n)}{E_1} + \sum_{k=2}^{n} \frac{I(\sum_{j=1}^{k} H_{je} - D_f, \nu_n) - I(\sum_{j=1}^{k-1} H_{je} - D_f, \nu_n)}{E_k} \right\} Bq \tag{23}$$

where

$$I(z, \nu) = K(0, \nu) - K(z, \nu) \tag{24}$$

and the equivalent thickness of equivalent single soil layer shown in Figure 2 is given by Equations (1) and (2).

Also, as for the immediate settlement in the centre of a foundation for multi-layered soil systems shown in Figure 1, a modified form of Odemark's method, which is referred to as the modified Odemark's method, is propounded in the following form:

$$S_i = \left\{ \frac{I(H_1 - D_f, \nu_1)}{E_1} + \sum_{k=2}^{n} \frac{I(\sum_{j=1}^{k} H_{je} - D_f, \nu_n) - I(\sum_{j=1}^{k-1} H_{je} - D_f, \nu_n)}{E_k} \right\} Bq \tag{25}$$

where the coefficients of correction, n_1 and n_2, represented in Odemark's method are assumed to be unity and the equivalent thickness of equivalent single soil layer shown in Figure 2 is designated by Equations (1) and (2).

For the immediate settlement in the centre of a foundation for multi-layered soil systems shown in Figure 3 and equivalent two-layered soil systems illustrated in Figure 4, the modified Palmer and Barber's method is represented in the following form:

$$S_i = [I(H_e - D_f, \nu_n)/E_H + \{I(H_e + H_n - D_f, \nu_n) - I(H_e - D_f, \nu_n)\}/E_n]Bq \tag{26}$$

Also, the modified Odemark's method is written as follows:

$$S_i = [I(H - D_f, \nu_n)/E_H + \{I(H_e + H_n - D_f, \nu_n) - I(H_e - D_f, \nu_n)\}/E_n]Bq \tag{27}$$

EQUIVALENT ELASTIC MODULI OF SEMI-INFINITE MULTI-LAYERS

Considering the case where a semi-infinite layer underlies the single layer with an equivalent elastic modulus as shown in Figure 4 in conditions that $H_n \to \infty$, circularly loaded area $B = 2a$, Poisson's ratio $\upsilon_n = 0.5$ and depth $D_f = 0$, Equations (26) and (27) are expressed, respectively, as follows:
for the modified Palmer and Barber's method:

$$S_i = \frac{1.5aq}{E_H} F_P \tag{28}$$

$$F_P = 1 - 1/\{1 + (H_e/a)^2\}^{1/2} + m/\{1 + (H_e/a)^2\}^{1/2} \tag{29}$$

DOI: 10.1002/nag

and for the modified Odemark's method:

$$S_i = \frac{1.5aq}{E_H} F_O \tag{30}$$

$$F_O = 1 - 1/\{1 + (H/a)^2\}^{1/2} + m/\{1 + (H_e/a)^2\}^{1/2} \tag{31}$$

where $m = E_H/E_n$ and the equivalent thickness is expressed by

$$E_H \geqslant E_n : H_e = (E_H/E_n)^{1/3} H \tag{32}$$

$$E_H < E_n : H_e = \{0.75 + 0.25(E_H/E_n)^{1/3}\} H \tag{33}$$

Assuming an equivalent semi-infinite layer for the system consisting of a single layer and a semi-infinite layer, we obtain the immediate settlement in the centre of a circular foundation in the following form:

$$S_i = \frac{1.5aq}{E_{\text{equ}}} \tag{34}$$

where E_{equ} denotes the equivalent elastic modulus of the equivalent semi-infinite layer. Therefore, it is seen from Equations (28)–(31) and (34) as follows:
for the modified Palmer and Barber's method:

$$E_{\text{equ}} = E_H/F_P \tag{35}$$

and for the modified Odemark's method:

$$E_{\text{equ}} = E_H/F_o \tag{36}$$

EXPRESSIONS OF VERTICAL STRESS

For the semi-infinite soil medium of the elastic modulus E_n and Poisson's ratio v_n subjected to uniform loads q on a rectangular foundation with the transverse dimension B and the longitudinal one L, the vertical stress at the depth z below the centre of foundation is expressed as follows [19, 20]:

$$\begin{aligned}\Delta\sigma'_{\text{v}} &= \Delta\sigma'_{\text{v}}(z) \\ &= \frac{2q}{\pi}\left[\frac{mn}{\sqrt{1+m^2+n^2}}\frac{1+m^2+2n^2}{(m^2+n^2)(1+n^2)} + \sin^{-1}\frac{m}{\sqrt{m^2+n^2}\sqrt{1+n^2}}\right]\end{aligned} \tag{37}$$

where $m = L/B$ and $n = 2z/B$.

As for the semi-infinite soil medium of the elastic modulus E_n and Poisson's ratio v_n subjected to uniform loads q on a circular foundation with radius a, the vertical stress at the depth z below

DOI: 10.1002/nag

the centre of foundation is written as follows [35, 48]:

$$\Delta\sigma'_{\mathrm{v}} = \Delta\sigma'_{\mathrm{v}}(z) = q\left[1 - \frac{1}{\left(1 + \dfrac{a^2}{z^2}\right)^{3/2}}\right] \tag{38}$$

For the vertical stress in each layer below the centre of foundation on multi-layered soil systems shown in Figure 1, substituting the sum of each equivalent thickness, which is given by Equation (1) and/or (2) and is illustrated in Figure 2, into the depth z in Equations (37) or (38), we obtain the vertical stress in each layer of multi-layered soil systems shown in Figure 1. For the vertical stress in each layer below the centre of foundation on improved soil systems shown in Figure 8, substituting the sum of each equivalent thickness, which is given by Equations (15)–(18) and is illustrated in Figure 14, into the depth z in Equations (37) or (38), we get the vertical stress in each layer of improved soil systems shown in Figure 8.

On the other hand, using the equation of equilibrium of vertical stress for multi-layered soil systems shown in Figure 1 leads to the vertical stress in each layer as follows:

$$\Delta\sigma'_{\mathrm{v}} = \left(\frac{B \cdot L}{B_{je} \cdot L_{je}}\right) q \tag{39}$$

Substituting the distribution widths of vertical stress defined by Equation (3), B_{je} and L_{je}, into Equation (39), we obtain the vertical stress in each layer of multi-layered soil systems shown in Figure 1. Employing the equation of equilibrium of vertical stress for improved soil systems shown in Figure 8 yields the vertical stress in each layer as follows:

$$\Delta\sigma'_{\mathrm{v}} = \left(\frac{B \cdot L}{B'_{je} \cdot L'_{je}}\right) q \tag{40}$$

Substituting the distribution widths of vertical stress defined by Equation (14), B'_{je} and L'_{je}, into Equation (40), we get the vertical stress in each layer of improved soil systems shown in Figure 8.

ANALYSES OF IMMEDIATE SETTLEMENT AND VERTICAL STRESS

Let us consider the immediate settlement and the vertical stress in two layers subjected to circular uniform load on the surface of soil medium where a single layer rests on a semi-infinite layer shown in Figure 16. Equations (23) and (25) are used to predict the immediate settlement in the following presentation. Poisson's ratios are assumed that $\upsilon_1 = \upsilon_2 = 0.5$. For two cases where $H_1 = a$ and $H_1 = 3a$ when $m = E_1/E_2 \leqslant 1$ and the equivalent thickness given by Equation (2) is adopted, Figures 17 and 18 exhibit relationships between m and the deflection factor F_s which is defined as $F_s = S_i/(2aq(1 - \upsilon_1^2)/E_1)$, where S_i is the immediate settlement on surface in the centre of foundation. The deflection factor F_s is the same as F_P and F_O indicated by Equations (29) and (31), respectively. The rigorous solutions presented by Himeno [33] and Matsui [34] are shown and are referred to simply as ELSA and GAMES, respectively. It is found that Palmer and Barber [24] method is not able to represent the rigorous solution in the range of small m, but Simons and Menzies [28] method, modified Palmer *et al.*'s method expressed by Equation (23)

DOI: 10.1002/nag

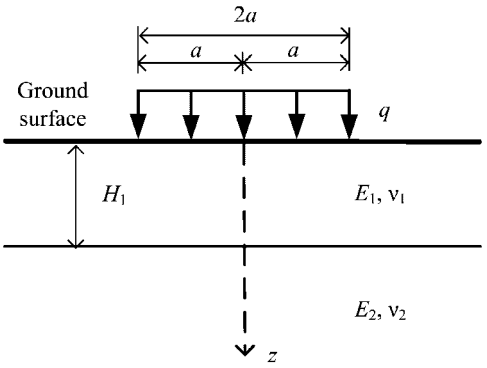

Figure 16. Two-layered soil systems under circular uniform loads on ground surface.

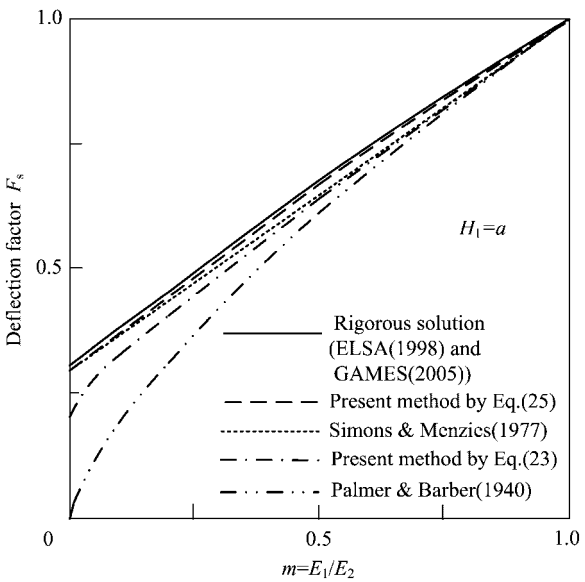

Figure 17. Relationships between elastic modulus and deflection factor.

and modified Odemark's method given by Equation (25) are capable of simulating the rigorous solution properly for the range that $m \leqslant 1.0$.

Figures 19 and 20 show relationships between m and the deflection factor F_s for two cases where $H_1 = a$ and $H_1 = 3a$ when $m = E_1/E_2 \geqslant 1$ and the equivalent thickness is given by Equation (1). In this case, the modified Palmer *et al.*'s method given by Equation (23) and the modified Odemark's method expressed by Equation (25) reduce to the Palmer *et al.*'s method and the Odemark's method, respectively. It is seen that Equations (23) and (25) are capable of describing the rigorous solution properly for the range that $m \geqslant 1.0$, but Simons *et al.*'s method cannot simulate the rigorous solution as m increases.

DOI: 10.1002/nag

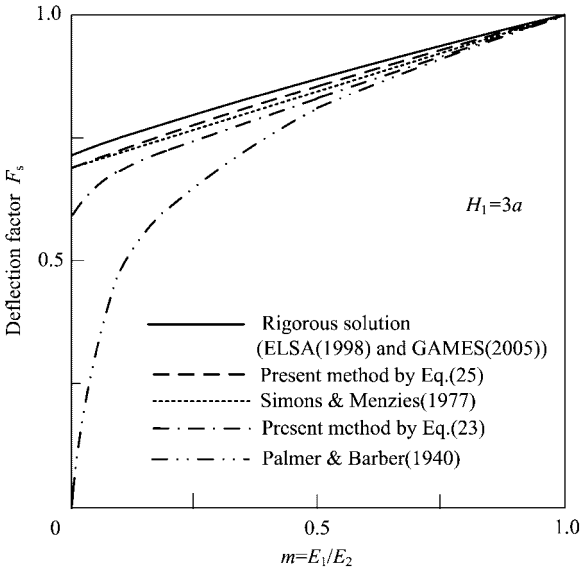

Figure 18. Relationships between elastic modulus and deflection factor.

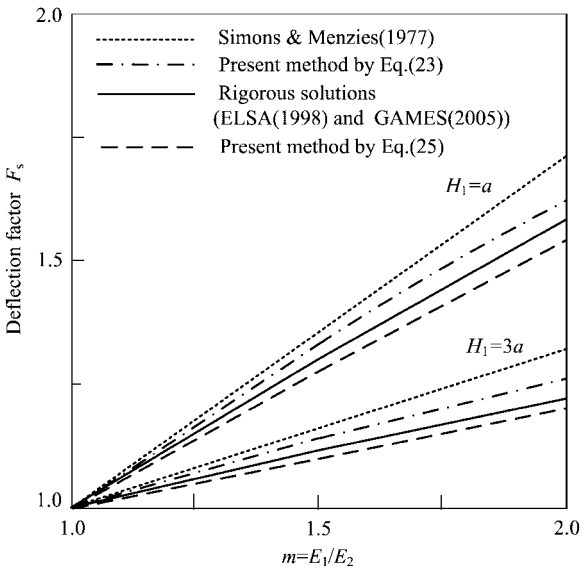

Figure 19. Relationships between elastic modulus and deflection factor.

Figures 21 and 22 exhibit relationships between m and the normalized vertical stress σ_z/q on the interface between upper and lower layers below the centre of circular foundation as shown in Figure 16 for two cases that $H_1 = a$ and $H_1 = 3a$ when Equation (38) is employed and Equations (1) and (2) of the equivalent thickness are specified according as $m \geqslant 1.0$ and $m \leqslant 1.0$, respectively. In comparison with the rigorous solutions calculated by ELSA and GAMES for two layers,

DOI: 10.1002/nag

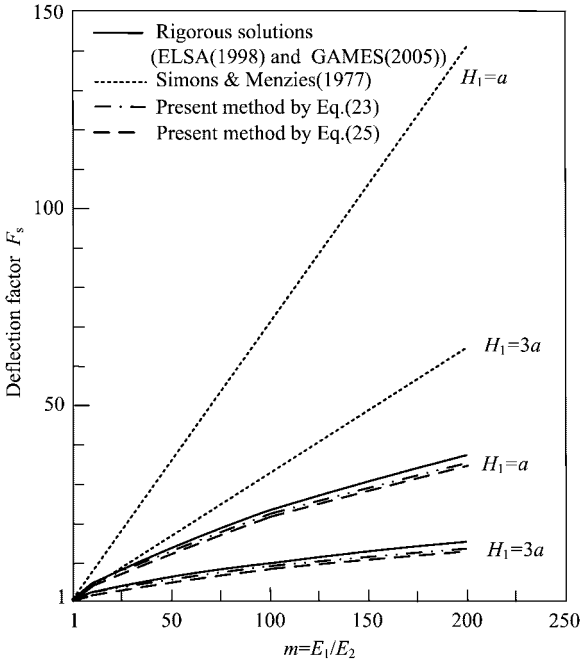

Figure 20. Relationships between elastic modulus and deflection factor.

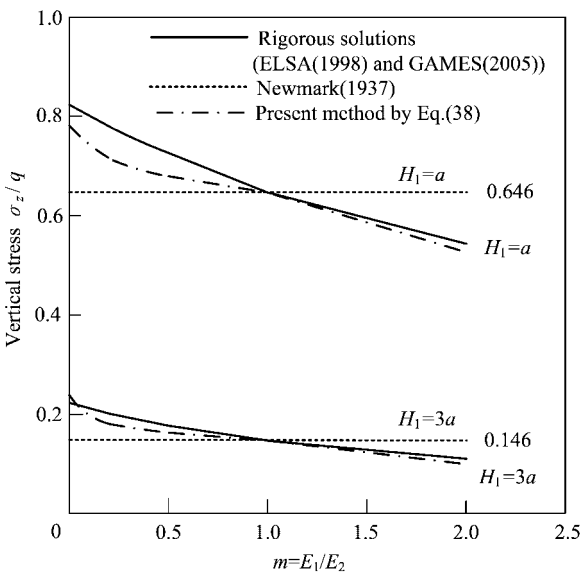

Figure 21. Relationships between elastic modulus and vertical stress

DOI: 10.1002/nag

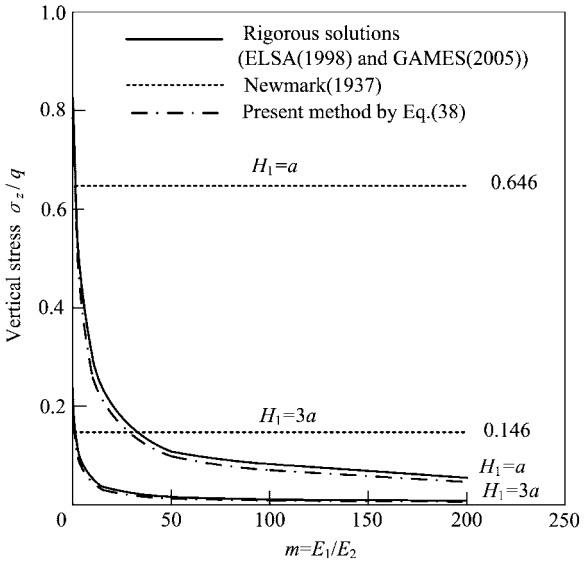

Figure 22. Relationships between elastic modulus and vertical stress.

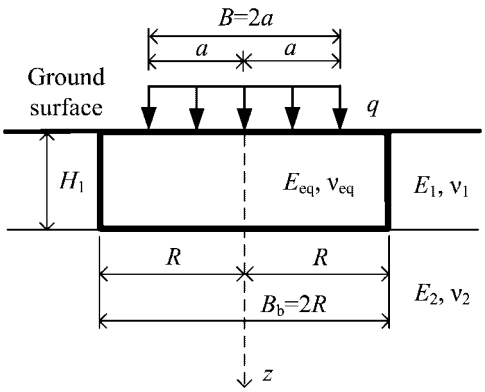

Figure 23. Improved soil systems under circular uniform loads on ground surface.

the proposed solutions given by Equation (38) with Equations (1) and (2) are able to simulate the behaviour of the vertical stress which decreases with the increase of m. For an isotropic and homogeneous medium where elastic moduli in two layers take equal values, the vertical stresses [48] possess constant values 0.646 and 0.146 for $H_1 = a$ and $H_1 = 3a$, respectively.

For improved soil systems shown in Figure 8, since the elastic soil parameters of improved soil systems can be experimentally determined, the equivalent elastic moduli given by Equation (7) are obtained easily. Because of this reason, we focus on the improved soil systems composed of a composite soil system and multi-layered soil systems exhibited in Figure 9.

Figure 23 shows that circular loads are provided on the surface of improved soil systems where both a composite soil system with E_{eq} and υ_{eq} and an external soil layer with E_1 and υ_1 overlie

DOI: 10.1002/nag

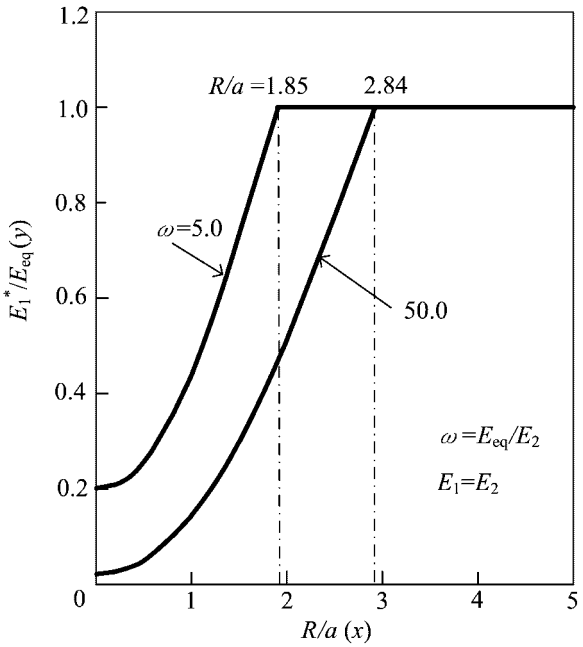

Figure 24. Relationships between length and equivalent elastic modulus.

a semi-infinite soil layer with E_2 and υ_2. It is assumed that Poisson's ratios take $\upsilon_1 = \upsilon_2 = \upsilon_{eq}$. Applying Equation (13) with Equations (7)–(12) to the case of Figure 23, we have

$$y = \xi + \frac{4(1-\xi)}{(2+\eta\omega^{1/3})^2}x^2 \tag{41}$$

where $y = E_1^*/E_{eq}$, $\xi = E_1/E_{eq}$, $\eta = H_1/a$, $\omega = E_{eq}/E_2$, $x = R/a$.

Figure 24 shows relationships between $x = R/a$ and $y = E_1^*/E_{eq}$ expressed by Equation (41) when $E_1 = E_2$ and $\eta = 1.0$. It is found that the equivalent elastic modulus E_1^* increases initially and takes constant value $E_1^*/E_{eq} = 1.0$ at $R/a = 1.85$ and 2.84 for $E_{eq}/E_2 = 5.0$ and 50.0, respectively, as the radius R increases.

In the following presentation, the proposed solutions of immediate settlement are calculated by the modified Palmer and Barber's method indicated in Equation (23) with Equations (7)–(18). For two cases that $E_{eq}/E_2 = 5.0$ and 50.0, Figures 25 and 26 show the relationships between $x = R/a$ and the deflection factor F which is defined as $F = w/(2aq(1-\upsilon_2^2)/E_2)$, where w is the immediate settlement on surface in the centre of foundation. It is assumed that $E_1 = E_2$, $\eta = 1.0$, $\upsilon_1 = \upsilon_2 = \upsilon_{eq}$ and Poisson's ratios take 0.3 and 0.5. Since the stiffness matrix in the FEM [49] represents infinity for Poisson's ratio = 0.5 in the case of axisymmetric elastic problems, Poisson's ratio = 0.49 is adopted approximately instead of 0.5. In Figure 25, it is found from the proposed solutions that as R/a increases, the deflection factor F decreases and after R/a reaches 1.85, the deflection factors for Poisson's ratios 0.3 and 0.5 keep constant values 0.55 and 0.61, respectively. It is seen from the proposed solutions in Figure 26 that as R/a increases, the deflection factor F decreases and after R/a reaches 2.84, the deflection factors for Poisson's ratios 0.3 and 0.5 retain

DOI: 10.1002/nag

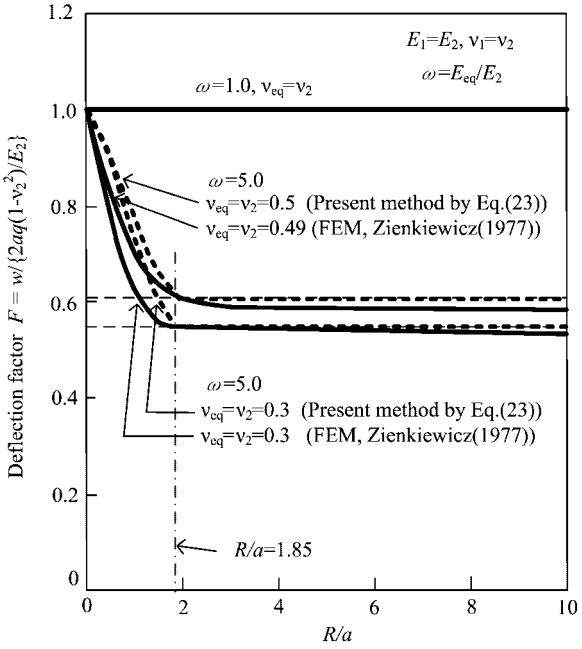

Figure 25. Relationships between length and deflection factor.

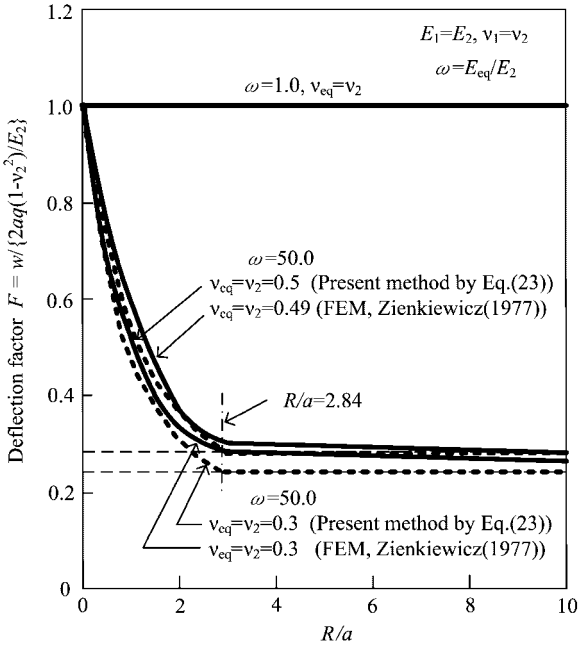

Figure 26. Relationships between length and deflection factor.

DOI: 10.1002/nag

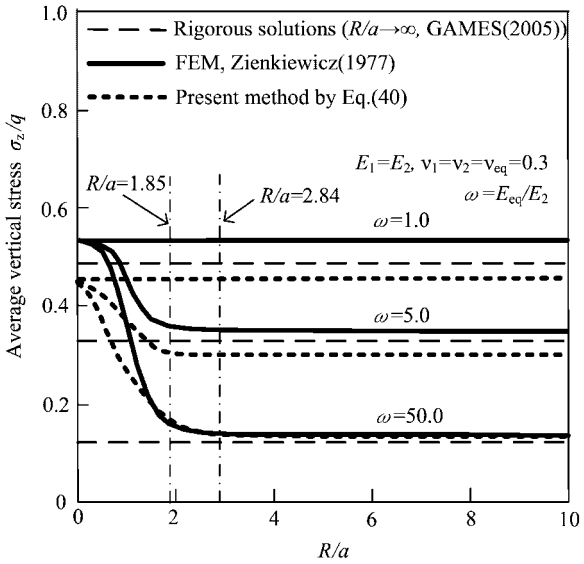

Figure 27. Relationships between length and average vertical stress.

constant values 0.24 and 0.28, respectively. On the other hand, the analyses by FEM represent the same tendencies as the proposed solutions.

Figure 27 shows the relationships between R/a and the normalized average vertical stress σ_z/q on the interface between the composite soil system and the lower soil layer exhibited in Figure 23. The analyses are performed by the proposed model given by Equation (40) with Equations (7)–(18) and the FEM is provided. It is assumed that $E_1 = E_2$, $\eta = 1.0$ and $\upsilon_1 = \upsilon_2 = \upsilon_{eq} = 0.3$. The rigorous solutions calculated by GAMES correspond to the results of two layers where R/a is infinite and it is observed that average vertical stresses σ_z/q take constant values 0.490, 0.333 and 0.120 for $E_{eq}/E_2 = 1.0$, 5.0 and 50.0, respectively. The proposed solutions represent the results as follows: (i) The average vertical stress σ_z/q for $E_{eq}/E_2 = 1.0$ has a constant value 0.444. (ii) As R/a increases, σ_z/q decreases and after R/a reaches 1.85 and 2.84, average vertical stresses σ_z/q keep constant values 0.292 and 0.124 for $E_{eq}/E_2 = 5.0$ and 50.0, respectively. On the other hand, the analyses by FEM indicate the same trends as the proposed solutions.

Figure 28 shows that circular loads are applied to the surface of improved soil systems where both a composite soil system with E_{eq} and υ_{eq} and an external soil layer with E_1 and υ_1 rest on the second layer with E_2 and υ_2 overlying a semi-infinite layer with E_3 and υ_3. It is assumed that $H_t = H_1 + H_2$, $H_t/a = 2.0$, $H_1/a = 1.2$, $E_2/E_3 = 2$, and $\upsilon_1 = \upsilon_2 = \upsilon_3 = \upsilon_{eq} = 0.5$ in Figure 28. Applying Equation (13) with Equations (7)–(12) to the case of Figure 28, we have

$$y = \xi + \frac{4(1-\xi)}{(2+\eta\omega^{1/3})^2}x^2 \tag{42}$$

where $y = E_1^*/E_{eq}$, $\xi = E_1/E_{eq}$, $\eta = H_1/a$, $\omega = E_{eq}/E_3$, $x = R/a$.

Figure 29 shows the relationships between $x = R/a$ and $y = E_1^*/E_{eq}$ expressed by Equation (42). It is found from Figure 29 that the equivalent elastic modulus E_1^* increases initially and takes

DOI: 10.1002/nag

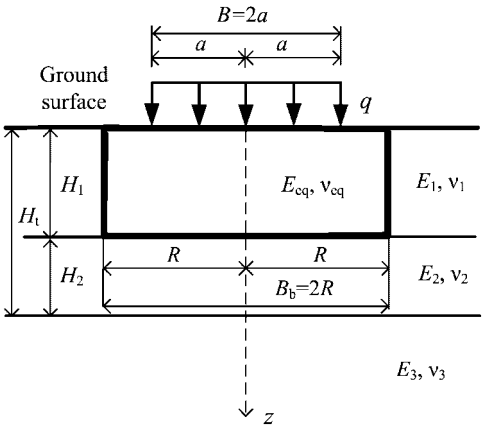

Figure 28. Improved soil systems under circular uniform loads on ground surface.

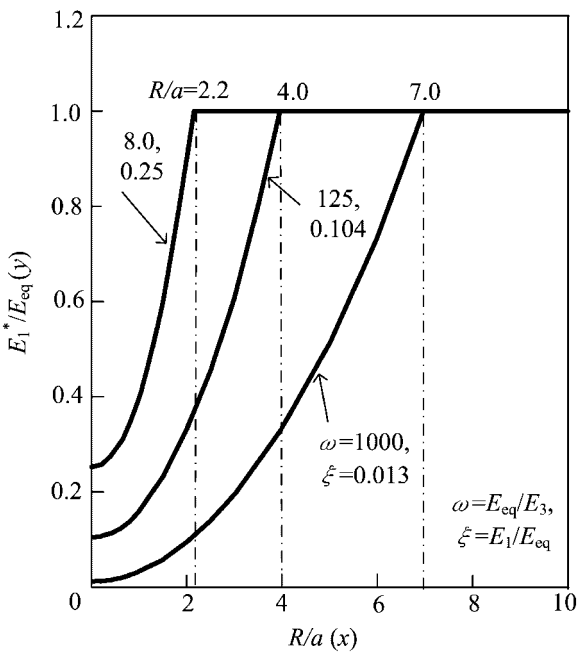

Figure 29. Relationships between length and equivalent elastic modulus.

constant value $E_1^*/E_{eq} = 1.0$ at $R/a = 2.2$, 4.0 and 7.0 for $(\omega, \xi) = (8.0, 0.25)$, $(125, 0.104)$ and $(1000, 0.013)$, respectively, as the radius R increases. Table I shows the equivalent elastic moduli E_1^* which are calculated by Equation (42) for the three cases in Figure 28.

In Figures 30–36, the investigation is achieved for equivalent three-layered soil systems such as Figure 13 into which improved soil systems illustrated in Figure 28 are transformed.

DOI: 10.1002/nag

Table I. Soil parameters for improved soil systems and equivalent three-layered soil systems.

	Case 1	Case 2	Case 3
R/a (x)	1.27	1.0	3.05
$E_{eq}/E_3(\omega)$	8	125	1000
E_1/E_3 $(\xi\omega)$	2	13	13
E_2/E_3	2	2	2
v_{eq}, v_1, v_2, v_3	0.5	0.5	0.5
E_1^*/E_{eq} (y)	0.5	0.16	0.2
E_1^*/E_3	4	20	200

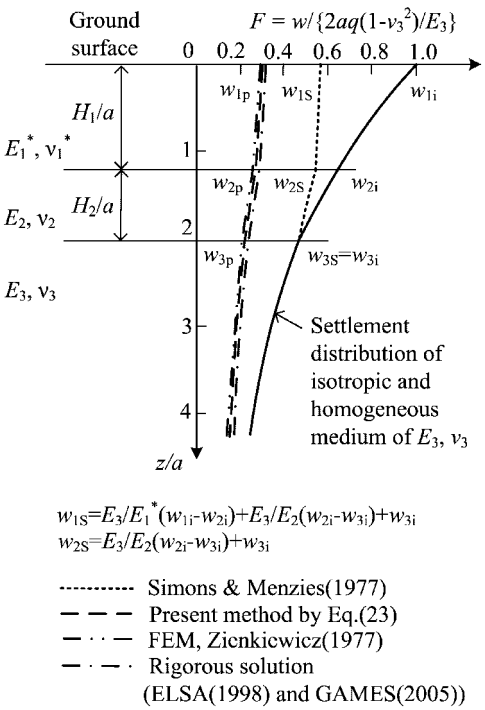

Figure 30. Settlement distributions at depth z/a in centre of foundation for Case 2.

Figure 30 exhibits the distributions of immediate settlement at depth z/a in centre of foundation for soil parameters of Case 2 shown in Table I. Equation (23) with Equations (7)–(18) is adopted. The deflection factor F is defined as $F = w/(2aq(1-\upsilon_3^2)/E_3)$, where w is the immediate settlement at depth z/a in the centre of foundation. It is found from Figure 30 that Simons *et al.*'s method is incapable of describing the rigorous solution given by ELSA and GAMES, but the proposed method as well as the FEM can represent the rigorous solution accurately.

DOI: 10.1002/nag

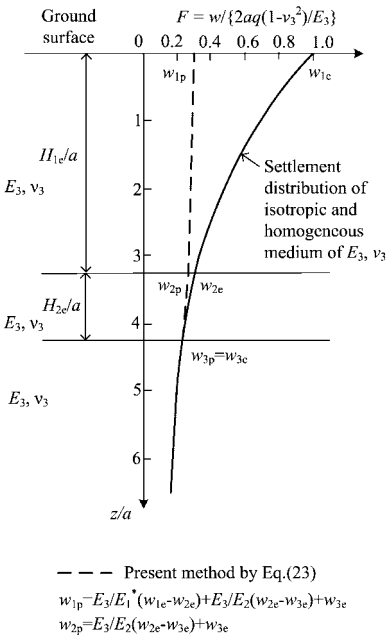

Figure 31. Proposed method to determine settlement distributions at depth z/a in centre of foundation for Case 2.

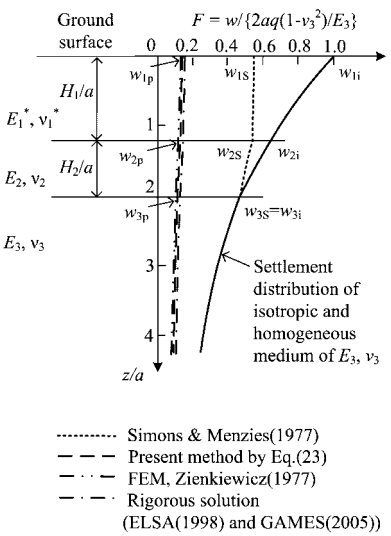

Figure 32. Settlement distributions at depth z/a in centre of foundation for Case 3.

DOI: 10.1002/nag

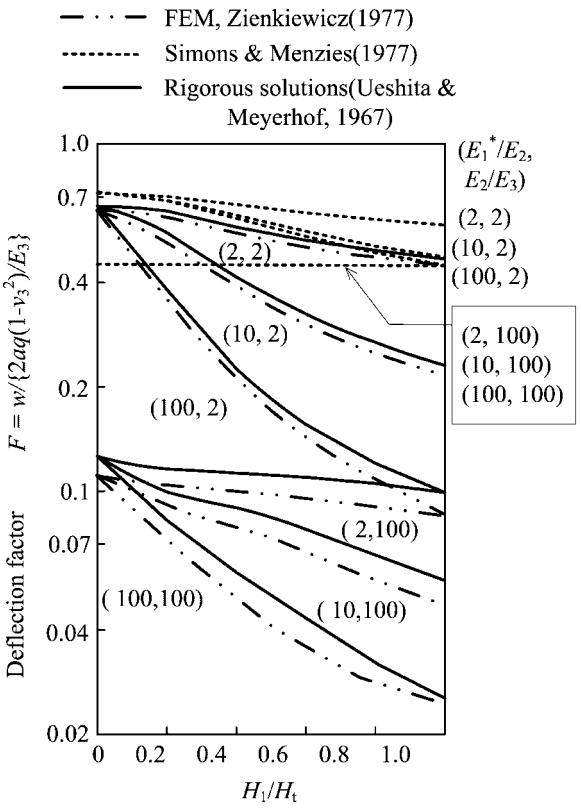

Figure 33. Relationships between thickness and deflection factor.

Figure 31 indicates the proposed procedure to determine the distribution of immediate settlement at depth z/a. As Figure 31 is a detailed description for the derivation of the proposed solution in Figure 30, Equation (23) with Equations (7)–(18) is used. The immediate settlements in multi-layered soil systems are obtained by taking into account the ratio of stiffness on the basis of the immediate settlement in the equivalent isotropic and homogeneous medium into which the multi-layered soil systems are transformed. The result simulated in Figure 31 provides the proposed solution illustrated in Figure 30.

Figure 32 exhibits the distributions of immediate settlement at depth z/a in the centre of foundation for soil parameters of Case 3 shown in Table I. Equation (23) with Equations (7)–(18) is adopted. The equivalent elastic modulus E_1^* of the first layer in Case 3 is greater than that in Case 2. It is found from Figure 32 that Simons *et al.*'s method is not able to describe the rigorous solution given by ELSA and GAMES, but the proposed method as well as the FEM can simulate the rigorous solution accurately.

Figures 33 and 34 show the relationships between ratio of thickness H_1/H_t and the deflection factor F, and it is assumed that $H_t = H_1 + H_2$, $H_t/a = 2.0$ and $\nu_1^* = \nu_2 = \nu_3 = 0.5$. Equation (23) with Equations (7)–(18) is used. The deflection factor F is defined as $F = w/(2aq(1 - \upsilon_3^2)/E_3)$, where w is the immediate settlement on surface in the centre of foundation. It is found in

DOI: 10.1002/nag

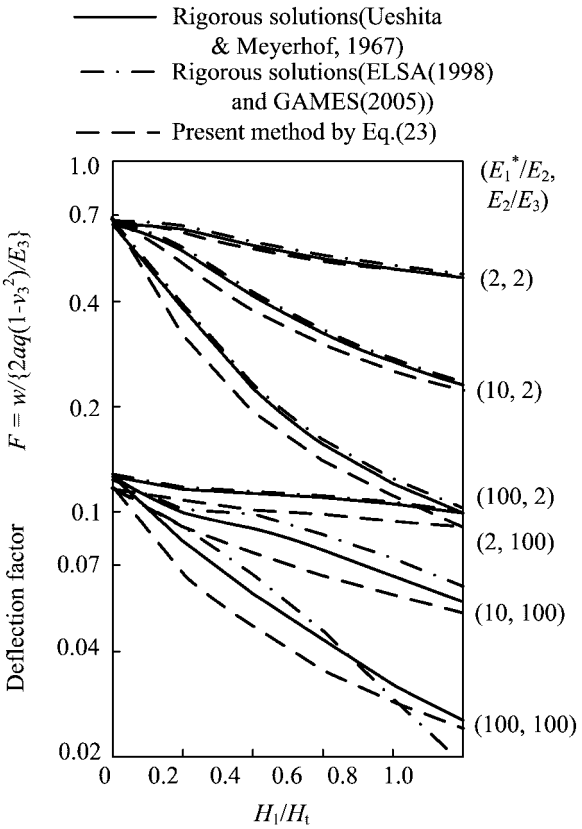

Figure 34. Relationships between thickness and deflection factor.

Figures 33 and 34 that compared with the rigorous solutions given by Ueshita and Mayerhof [21, 22], ELSA and GAMES, Simons *et al.*'s method is incapable of predicting rigorous solutions, however, the FEM and the proposed method can describe the tendency of rigorous solutions accurately.

Figure 35 shows the relationships between ratio of stiffness E_2/E_3 and the normalized vertical stress σ_{z2}/q in the centre of interface between the second and the third layers for the case where $a/H_2 = 1.0$, $H_1/H_2 = 1.0$ and $\nu_1^* = \nu_2 = \nu_3 = 0.5$. Figure 36 exhibits the relationships between ratio of length a/H_2 and the normalized vertical stress σ_{z2}/q in the centre of interface between the second and the third layers for the case where $H_1/H_2 = 1.0$, $E_2/E_3 = 2.0$ and $\nu_1^* = \nu_2 = \nu_3 = 0.5$. Equations (38) and (40) with Equations (7)–(18) are employed. It is found from Figures 35 and 36 that compared with the rigorous solutions given by Jones [17], ELSA and GAMES, Newmark's [48] solution for an isotropic and homogeneous elastic medium is not able to predict the rigorous solutions; however, two proposed solutions given by Equations (38) and (40) can describe the tendency of rigorous solutions accurately.

For the above-mentioned equations employed in the equivalent elastic method, Table II shows the summary of formulae related to each figure of Figures 1–36.

DOI: 10.1002/nag

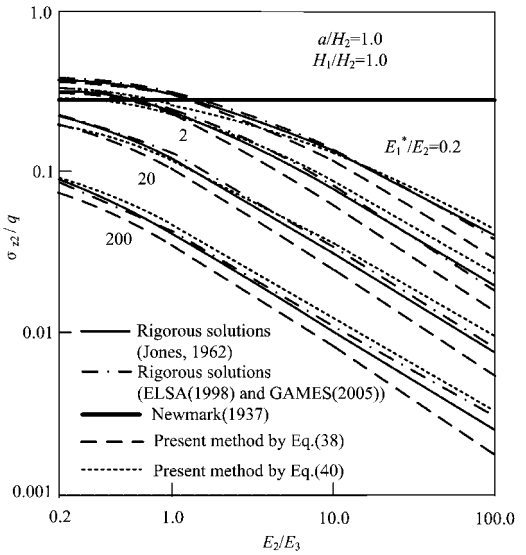

Figure 35. Relationships between elastic modulus and vertical stress.

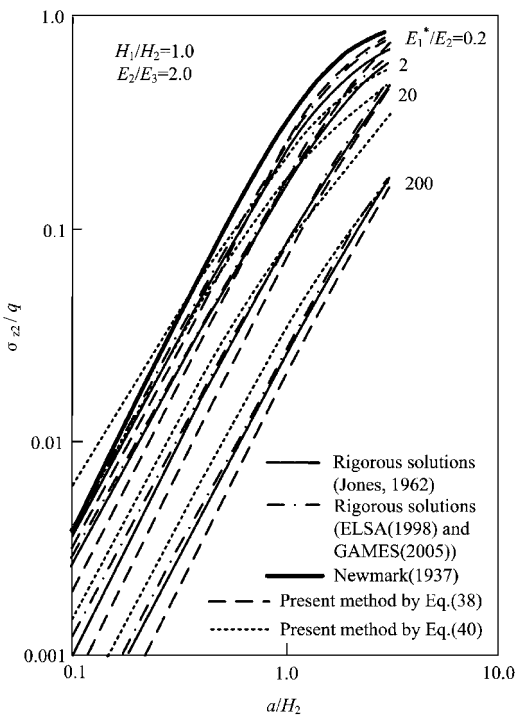

Figure 36. Relationships between length and vertical stress.

DOI: 10.1002/nag

Table II. Summary of formulae presented.

Figures	Equations related to each figure
1 and 2	Equations (1)–(3)
3–5	Equations (4)–(6)
6–10	Equation (7)
11	Equations (7)–(12)
12	Equations (7)–(12)
13	Equation (13)
14	Equations (13)–(18)
15	Equations (13)–(18)
16	Equations (23), (25) and (38)
17	Equations (23) and (25) with Equation (2)
18	Equations (23) and (25) with Equation (2)
19	Equations (23) and (25) with Equation (1)
20	Equations (23) and (25) with Equation (1)
21	Equation (38) with Equations (1) and (2)
22	Equation (38) with Equations (1) and (2)
23	Equations (23) and (40) with Equations (7)–(18)
24	Equation (41) derived from Equation (13) with Equations (7)–(12)
25	Equation (23) with Equations (7)–(18)
26	Equation (23) with Equations (7)–(18)
27	Equation (40) with Equations (7)–(18)
28	Equations (23), (38) and (40) with Equations (7)–(18)
29	Equation (42) derived from Equation (13) with Equations (7)–(12)
30	Equation (23) with Equations (7)–(18)
31	Equation (23) with Equations (7)–(18)
32	Equation (23) with Equations (7)–(18)
33	Equation (23) with Equations (7)–(18)
34	Equation (23) with Equations (7)–(18)
35	Equations (38) and (40) with Equations (7)–(18)
36	Equations (38) and (40) with Equations (7)–(18)

CONSOLIDATION SETTLEMENT

The consolidation settlement for cohesive soils is written as follows:

$$S_c = \frac{C_s H}{1+e_0}\log_{10}\left(\frac{\sigma'_{vc}}{\sigma'_{v1}}\right) + \frac{C_c H}{1+e_0}\log_{10}\left(\frac{\sigma'_{v1}+\Delta\sigma'_v}{\sigma'_{vc}}\right) \tag{43}$$

where C_s is the swelling index, C_c the compression index, H the thickness of layer, e_0 the void ratio, σ'_{v1} the effective vertical stress prior to construction, σ'_{vc} the consolidation yield stress, $\Delta\sigma'_v$ the increment of effective vertical stress.

Substituting vertical stresses calculated in Equations (37)–(40) as increments of effective vertical stress into Equation (43), we obtain consolidation settlements classified as elastic–plastic deformation for multi-layered soil systems and improved soil systems.

DOI: 10.1002/nag

CONCLUSIONS

The following conclusions were drawn from the present investigation:

1. Since the equivalent thickness presented by Palmer and Barber can be adopted only for the case where the elastic modulus of the upper layer is greater than that of lower one in two layers, the proposal of the equivalent thickness is made for the case where the elastic modulus of the upper layer is smaller than that of lower one in two layers.
2. For the multi-layer theory of elasticity, as the equivalent thickness offered by Odemark is available only for the case where the elastic moduli decrease with depth, the equivalent thickness is proposed for the case where the elastic moduli increase with depth.
3. Since each representation of immediate settlement provided by Palmer *et al.* and Odemark can be used only for the case where the elastic moduli decrease with depth, the proposals of immediate settlement for the case where the elastic moduli increase with depth are made by use of the equivalent thickness which is derived from Terzaghi's formula of the vertical stress. The proposed formulations of immediate settlement are referred to as the modified Palmer and Barber's method and the modified Odemark's method.
4. In order to generalize the formula of vertical stress on a rigid layer indicated by Terzaghi, expressions of vertical stress for multi-layers are proposed by use of the equivalent thickness and distribution widths of vertical stress.
5. It is verified that the extrapolation of Steinbrenner's approximation given by Simons *et al.* is not able to represent the rigorous solutions of the settlement for the case where the elastic moduli decrease with depth for the multi-layers.
6. In order to describe the heterogeneous elastic properties of multi-layered soil systems with soil improvement, analytical models are proposed by employing the hydrid method which consists of equivalent elastic modulus and equivalent thickness.
7. Since improved soil systems are reduced to the equivalent multi-layered soil systems, the proposed method for multi-layered soil systems is applicable to the improved soil systems. The modified Palmer and Barber's method and the modified Odemark's one are available for immediate settlements of multi-layered soil systems with soil improvement. The good agreement of immediate settlements is observed between the rigorous solutions and the simulation results.
8. Expressions of the vertical stress of multi-layered soil systems with soil improvement are proposed by using both the method of adopting equivalent thickness directly and the method of taking into account distribution widths of vertical stress. The comparison of vertical stresses between simulation results and rigorous solutions provides the reasonable agreement.

REFERENCES

1. Hirai H. An elastoplastic constitutive model for cyclic behaviour of sands. *International Journal for Numerical and Analytical Methods in Geomechanics* 1987; **11**:503–520.
2. Hirai H. Modelling of cyclic behaviour of sand with combined hardening. *Soils and Foundations* 1987; **27**(2):1–11.
3. Hirai H. A combined hardening model for anisotropically consolidated clays. *Soils and Foundations* 1989; **29**(3):14–24.
4. Kamei T, Hirai H. An elasto-viscoplastic model with combined hardening of anisotropically consolidated cohesive soils. *Soils and Foundations* 1990; **30**(2):89–102.
5. Hirai H, Kamei T. A combined hardening model of anisotropically consolidated cohesive soils. *Canadian Geotechnical Journal* 1991; **28**(1):1–10.

DOI: 10.1002/nag

6. Hirai H, Takahashi M, Yamada M. An elastic–plastic constitutive model for the behavior of improved sandy soils. *Soils and Foundations* 1989; **29**(2):69–84.
7. Architectural Institute of Japan. *Recommendations for Design of Building Foundations* (1st edn). Architectural Institute of Japan: Tokyo, Japan, 1988; 117–162.
8. Architectural Institute of Japan. *Recommendations for Design of Building Foundations* (2nd edn). Architectural Institute of Japan: Tokyo, Japan, 2001; 93–171.
9. Burmister DM. The theory of stresses and displacements in layered systems and applications to the design of airport runways. *Proceedings of HRB* 1943; **23**:126–148.
10. Burmister DM. The general theory of stresses and displacements in layered systems. *Journal of Applied Physics* 1945; **16**(2,3,5).
11. Burmister DM. Stress and displacement characteristics of a two-layer rigid base soil system: influence diagrams and practical application. *Proceedings of HRB* 1956; **35**:773–814.
12. Burmister DM. Evaluation of pavement systems of the WASHO road test by layered system methods. *Highway Research Board Bulletin* 1958; **177**:26–54.
13. Burmister DM. Applications of layered system concepts and principles to interpretations and evaluations of asphalt pavement performances and to design and construction. *Proceedings of the International Conference on Structural Design of Asphalt Pavements*, University of Michigan, 1962; 441–453.
14. Fox L. Computation of traffic stresses in a simple road structure. *Proceedings of the 2nd International Conference on Soil Mechanics and Foundation Engineering* 1948; **2**:236–246.
15. Schiffman RL. The numerical solution for stresses and displacements in a three-layer soil system. *Proceedings of the 4th International Conference on Soil Mechanics and Foundation Engineering* 1957; **2**:169–173.
16. Kirk JM. Beregning af nedsyningen i lagdelte systemer. *Dansk Vejtidsskrift* 1961; **38**(2):294–296.
17. Jones A. Tables of stresses in three-layer elastic systems. *Highway Research Board Bulletin* 1962; **342**:176–214.
18. Ueshita K, Meyerhof GG. Surface displacement of soil-rock systems under uniformly distributed loads. *Proceedings of the Japan Society of Civil Engineers* 1967; **143**:9–15.
19. Steinbrenner W. Tafeln zur Setzungsberechnung. *Die Straße* 1934; **1**:221.
20. Steinbrenner W. *Bodenmechanik und neizeitlicher Straßenbau*. Symposium by 24 authors. Volk und Reich Verlag: Berlin, 1936.
21. Ueshita K, Meyerhof GG. Elastic displacement of multi-layer soil systems. *Proceedings of the Japan Society of Civil Engineers* 1967; **144**:20–26.
22. Ueshita K, Meyerhof GG. Deflection of multilayer soil systems. *Journal of Soil Mechanics and Foundation Division* (ASCE) 1967; **93**(SM5):257–282.
23. Odemark N. *Investigations as to the Elastic Properties of Soils and Design of Pavements According to the Theory of Elasticity*, vol. 77. Statens Vaginstitute: Meddelande, Stockholm, Sweden, 1949.
24. Palmer LA, Barber ES. Soil displacement under a circular loaded area. *Proceedings of the Highway Research Board* 1940; **20**:279–286.
25. Nascimento U, Seguro JM, da Costa E, Pinela S. A method of designing pavements for road and airports. *Proceedings of the 5th International Conference on Soil Mechanics and Foundation Engineering* 1961; **2**: 283–288.
26. Ullidtz P. *Modelling Flexible Pavement Response and Performance*. Narayana Press: Odder, Denmark, 1998.
27. Freeman RB, Harr ME. Stress predictions for flexible pavement systems. *Journal of Transportation Engineering* (ASCE) 2004; **130**(4):495–502.
28. Simons NE, Menzies BK. *A Short Course in Foundation Engineering*. Newnes-Butterworth: London, 1977; 30–48.
29. Fraser RA, Wardle LJ. Numerical analysis of rectangular rafts on layered foundations. *Géotechnique* 1976; **26**(4):613–630.
30. Poulos HG, Davis EH. *Pile Foundation Analysis and Design*. Wiley: New York, 1980; 95–96.
31. Hirai H, Kamei T. A method to calculate settlement, stress and allowable stress of multi-layered ground. *Journal of Structural and Construction Engineering* 2003; **573**:81–88.
32. Hirai H, Kamei T. A method to calculate settlement, stress, failure and allowable stress of multi-layered ground by equivalent thickness theory. *Journal of Structural Construction Engineering* 2004; **581**:79–86.
33. Himeno K. *Elastic Layer System Analysis*. Department of Civil Engineering, Chuo University: Japan, 1998.
34. Matsui K. *Introduction to Pavement Structural Analysis Based on Multi-layered Elastic Systems—Application With GAMES* (*general analysis of multi-layered elastic systems*), *Pavement Engineering Library* 3. Japan Society of Civil Engineers, 2005.

DOI: 10.1002/nag

35. Terzaghi K. *Theoretical Soil Mechanics*. Wiley: New York, 1943.
36. Hirai H, Kamei T. A proposal of estimation of consolidation yield stress of cohesive soils. *Japanese Geotechnical Journal* 2002; **50**(5):11–13.
37. Hirai H, Kamei T. A proposal for estimation of allowable stress of ground by sounding test. *Journal of Structural and Construction Engineering* 2002; **557**:113–120.
38. Hirai H, Satake M. Stress analysis of a penny-shaped crack located between two spherical cavities in an infinite solid. *Journal of Applied Mechanics*, *Transactions of the ASME* 1980; **47**(4):806–810.
39. Hirai H, Satake M. Stress analysis of a penny-shaped crack located between two oblate spheroidal cavities in an infinite solid. *International Journal of Engineering Science* 1981; **19**:1283–1291.
40. Kögler F, Scheidig A. Druckverteilung im Baugrunde. *Die Bautechnik* 1927, 1928, 1929; **5–7**.
41. Yamaguchi H. Practical formula of the bearing value for two layered ground. *Proceedings of the 2nd Asian Regional Conference SMFE* 1963; **1**:176–180.
42. Randolph MF. Design methods for pile groups and piled rafts. *Proceedings of the 13th ICSMFE* 1994; **5**:61–82.
43. Hirai H, Kamei T. A method to calculate allowable stress and settlement of improved ground. *Proceedings of the 48th Symposium on Geotechnical Engineering*, The Japanese Geotechnical Society, 2003; 37–44.
44. Hirai H, Kamei T. A method to analyze settlement and stress of improved ground by equivalent elastic theory. *Proceedings of the Symposium on Research*, *Design*, *Execution Method and Evaluation of Properties for Soils Mixed with Cement and Cement-stabilizer*, The Japanese Geotechnical Society, 2005; 319–326.
45. Schleicher F. *Bauingenieur* 1926; **7**.
46. Love AEH. The stress produced in a semi-infinite solid by pressure on part of boundary. *Philosophical Transactions of the Royal Society of London*, *Series A* 1929; **228**.
47. Harr ME. *Foundations of Theoretical Soil Mechanics*. McGraw-Hill: New York, 1966.
48. Newmark NM. *Chart for Computing Vertical Pressures Beneath a Surface Loading*. University of Illinois, Illinois, 1937.
49. Zienkiewicz OC. *The Finite Element Method* (3rd edn). McGraw-Hill: U.K., 1977; 119–134.

DOI: 10.1002/nag